INTERNATIONAL JOURNAL FOR NUMERICAL METHODS IN FLUIDS, VOL. 17, 401–416 (1993)

FINITE ELEMENT ANALYSIS OF LIFT BUILD-UP DUE TO AEROFOIL INDICIAL MOTION

JUN SHI* AND DENNIS HITCHINGS

Department of Aeronautics, Imperial College, London SW7 2AZ, U.K.

SUMMARY

In this paper the problem of impulsively started aerofoil or sudden change of incidence of an aerofoil in incompressible potential flow is investigated. The essence of solution lies in the representation of a timely and spatially varying wake in a largely irrotational potential flow field. This is achieved by representing the wake through velocity potential difference, which seems to be the only way of imposing a velocity difference condition in the finite element context with velocity potentials as the basic unknowns. Superposition is employed to meet various boundary conditions, which is justified by the linearity of the problem. The finite element solutions are compared with those from singularity method.

KEY WORDS Finite element method Aerofoil indicial motion

1. INTRODUCTION

The aerodynamic force build-up on an aerofoil performing indicial motion is a problem of fundamental interest in unsteady aerodynamics. The subcritical response of an aeroplane in accelerated motion, such as the fast maneuver of a military aircraft or active controls, requires a theory of general time-dependent aerodynamics.[1] The aerodynamic force of arbitrary aerofoil motion can be derived from such forces of indicial motion by the convolution integral. Another approach is built on the reciprocal relation between indicial and oscillatory motions,[2] since with mild restriction on continuity and differentiability an arbitrary function can be expanded into a Fourier series.[3] Consequently, if we know the solution for oscillatory aerofoil motion over a wide range of frequencies, then, due to the linearity of the problem, they can be superposed in a truncated range of frequency to make up the solution for arbitrary aerofoil motion. However, this is an expensive process because the number of frequency points required to form a desired solution is normally large.

The indicial motion of an aerofoil can be categorized as the sudden change of heaving rate and pitching rate or the sudden change of incidence and control deflection (see Figure 1(a)–(d)). They are similar in essence, so only the sudden change of incidence which is also known as the impulsively started aerofoil, is explained in more detail below. A highly idealized example of an indicial problem is that an aerofoil in a uniform flow field suddenly changes its incidence. This is equivalent to the problem of an aerofoil stationary in still air at one instance of time but gains a non-zero speed at next instance. As the flow field is inviscid and initially circulation-free,

* Please send all future correspondence to: Dr. Jun Shi, Dept. of Aeronautics, The Queen's University of Belfast, Belfast BT9 5AG, Northern Ireland, Tel: 0232 245133, Fax: 0232 382701.

0271–2091/93/170401–16$13.00

Received June 1992
Revised April 1993

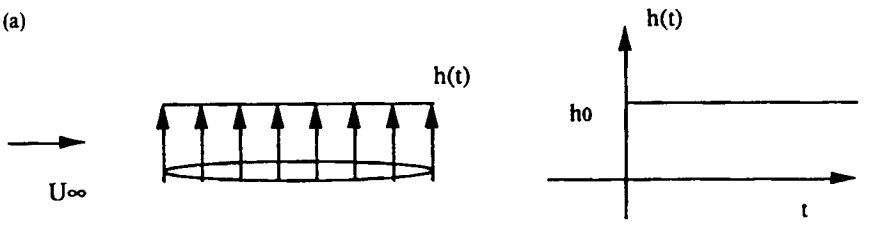

Figure 1(a). Step change of heaving rate

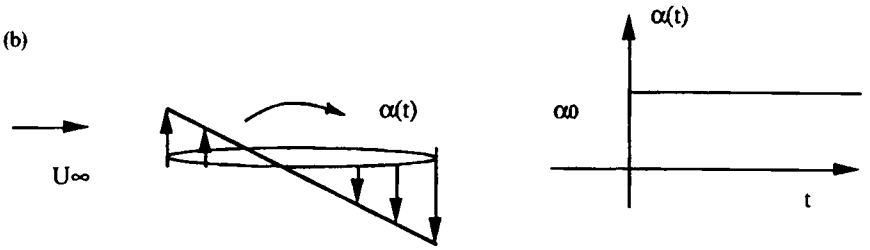

Figure 1(b). Step change of pitching rate

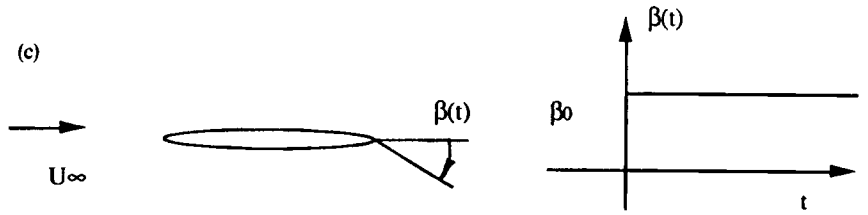

Figure 1(c). Step change of control surface deflection

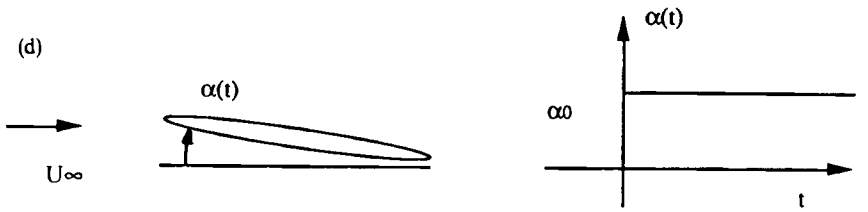

Figure 1(d). Step change of incidence

circulation should remain zero subsequently according to the Kelvin's law of conservation. Despite that the circulation of the whole flow field is zero, circulation or lift on the aerofoil increases as time develops accompanied by vortices of opposite sign shed from aerofoil to compensate for the increase of circulation on the aerofoil (Figure 2). These rotating fluid elements form a wake starting from the trailing edge of the aerofoil and they are the only part of the flow field that is rotational. For a more detailed discussion, the reader is referred to Batchelor.[4]

The original work in this field was done on a plate by Wagner.[5] To include the effect of thickness, deformation of wake and large motion amplitude, Giesing[6] and Basu[7] developed an

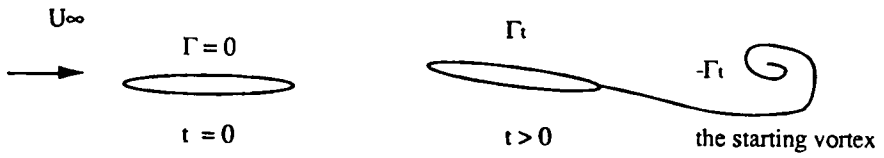

Figure 2. The lift build-up mechanism

unsteady Smith[8] method. They allowed the strength of the vorticity on the aerofoil surface to vary with time to accommodate vortex shedding. The solution is carried out in time domain by a time-marching method. The position of each vortex that has been shed is determined by the whole flow system at the last time instance.

Despite of the advantages of finite element over the boundary integral method,[9, 10] a finite element approach for this problem does not exist. In the following sections of this paper a finite element implementation is proposed to fill this gap. The approach advocated is general and not necessarily restricted to the present problem. It can be easily incorporated into an existing finite element package and provides a competitive alternative to the boundary integral method. In Section 3 an explicit time integration scheme is given with discussion on time-step selection in Section 4. In Section 5 numerical examples are presented and compared with those from other sources.

2. FINITE ELEMENT FORMULATION FOR INDICIAL AEROFOIL MOTION

To put the aforementioned phenomenon mathematically, let us define a velocity potential ϕ in Ω, where Ω is a fluid domain that encompasses the aerofoil but excludes the wake, as shown in Figure 3. Since the flow is assumed to be incompressible and irrotational except for the wake, the velocity potential ϕ must satisfy the Laplace equation plus various boundary conditions:

$$\begin{aligned} &\nabla^2\phi = 0 && \text{in } \Omega, \\ &\frac{\partial\phi}{\partial\mathbf{n}} = \mathbf{u}_\infty \mathbf{n} && \text{on } \partial\Omega_1, \\ &\frac{\partial\phi}{\partial\mathbf{n}} = f && \text{on } \partial\Omega_2, \\ &\Delta\phi = \Delta\phi(s, t) && \text{on } \partial\Omega_3, \end{aligned} \tag{1}$$

where $\mathbf{n}$ is the normal to the boundary and f a known function determined by the aerofoil motion. Note that $\partial\Omega_3$ is in fact a double surface of zero thickness.

As in Hitchings[11] and Shi,[12, 13] we have replaced the common velocity difference boundary condition on the wake with the velocity potential difference condition, because such a form of boundary condition can be easily accommodated in a finite element model, which will be discussed later. Since the finite element discretization of the Laplace equation has been fully explained elsewhere,[12, 14] the key issue is how to simulate the rotational wake in a finite element context. The wake in the present problem is different from the wake of an oscillating aerofoil addressed in Hitchings[11] and Shi,[12] where the wake is actually in a steady state. In this paper it is the transient development of the wake that is of concern.

The wake is assumed to be straight, infinitely thin and aligned with streamline at infinity exactly as in Hitchings[11] and Shi.[13] Consequently, the non-linearity coming from wake deformation is not included. The shed vortex is assumed to be convected at the free stream velocity, so

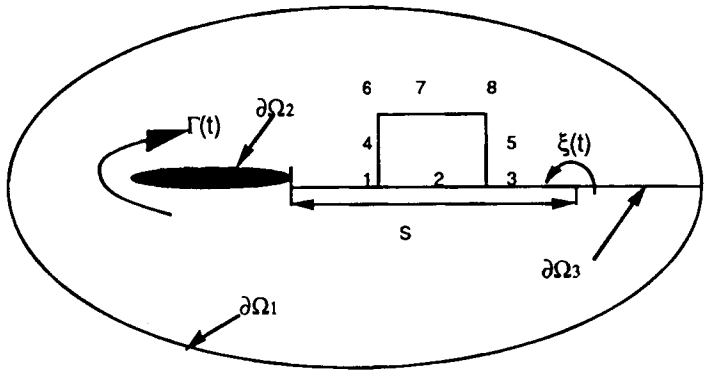

Figure 3. Problem definition of aerofoil indicial motion

that the strength of the vorticity at time t and position s is

$$\xi(s, t)=\frac{1}{U_\infty}\frac{\partial\Gamma(t-s/u_\infty)}{\partial t}, \tag{2}$$

where $\Gamma(t)$ is the circulation around the aerofoil. Note that the actual vorticity is actually the strength of vorticity per unit length, as we are dealing with an infinite thin vortex wake.

The velocity potential difference $\Delta\phi$ at a pair of points immediately above and below the wake can be found by integrating the velocity along the wake $\partial\Omega_3$ and the aerofoil surface $\partial\Omega_2$ in the same way as described in Hitchings:[11]

$$\begin{aligned}\Delta\phi(t, s)&=\int_{\partial\Omega_1+\partial\Omega_2}(U\,\mathrm{d}x+V\,\mathrm{d}y)\\&=\Gamma(t)+\int\xi(s, t)\,\mathrm{d}s \quad (0\le s\le U_\infty t)\\&=0 \qquad\qquad\qquad (s\ge U_\infty t).\end{aligned} \tag{3}$$

However, we can see that equation (3) is different from the corresponding equations in Hitchings[11] and Shi.[13] Firstly, since no assumption has been made about the circulation on the aerofoil, the variation of the circulation or the vorticity $\xi(s, t)$ from equation (2) is not explicitly given; secondly the problem is solved in the time domain rather than in the frequency domain. Therefore, the strength and the length of the wake depend upon time and only the part of $\partial\Omega_3$ already reached by the wake front ($s<U_\infty t$) has non-zero $\Delta\phi$; otherwise, $\Delta\phi=0$.

Now we will illustrate how to solve equation (1) with focus on the boundary condition as in equation (3). ϕ is interpolated as $\phi=N_i\phi_i$ on each non-overlapping subdomain (Ω_e and $\partial\Omega_e$) or element. Equation (1) weighted by W_i is integrated by part, which for a 2D problem gives

$$\int_\Omega\left(\frac{\partial W_j}{\partial x}\frac{\partial N_i}{\partial x}+\frac{\partial W_j}{\partial y}\frac{\partial N_i}{\partial y}\right)\phi_i\,\mathrm{d}\Omega=\oint_{\partial\Omega_e}W_i\left(\frac{\partial N_i}{\partial x}\mathrm{d}y-\frac{\partial N_i}{\partial y}\mathrm{d}x\right)\phi_i. \tag{4}$$

Special treatment is needed for those elements either above or below the wake, because of the boundary condition imposed by the wake. For easiness of discussion we consider an eight-node

quadrilateral element with the interpolation of the potential:

$$\phi = \sum_{i=1}^{8} N_i \phi_i, \tag{5}$$

where N_i are the element shape functions and ϕ_i are the nodal potentials.

For those elements on the upper surface of the slit (see Figure 3), if the nodal variables under the wake ϕ_k^- are chosen as basic unknowns, then those above the wake ϕ_k^+ are the sum of $\Delta\phi_k$ and ϕ_k^-:

$$\begin{aligned}\phi &= \sum_{i=4}^{8} N_i \phi_i^+ + \sum_{k=1}^{3} N_k(\phi_k^- + \Delta\phi_k) \\ &= \sum_{i=1}^{8} N_i \phi_i + \sum_{k=1}^{3} N_k \Delta\phi_k.\end{aligned} \tag{6}$$

This results in a slight modification in formulating the element matrix for those elements sitting above the wake and for $s < U_\infty t$ (see Figure 3):

$$\begin{aligned}\int_{\Omega_e}\left(\frac{\partial W_j}{\partial x}\frac{\partial N_i}{\partial x}+\frac{\partial W_j}{\partial y}\frac{\partial N_i}{\partial y}\right)\phi_i \,d\Omega &= \oint_{\partial\Omega_e} W_j\left(\frac{\partial N_i}{\partial x}dy - \frac{\partial N_i}{\partial y}dx\right)\phi_i \\ &\quad - \sum_{k=1}^{3}\int_{\Omega_e}\left(\frac{\partial W_j}{\partial x}\frac{\partial N_k}{\partial x}+\frac{\partial W_j}{\partial y}\frac{\partial N_k}{\partial y}\right)\Delta\phi_k \,d\Omega \quad (i, j = 1, 2, \ldots, 8)\end{aligned} \tag{7}$$

or in a matrix form

$$\mathbf{C}_e \boldsymbol{\Phi}_e = \mathbf{f}_1 + \mathbf{f}_2, \tag{8}$$

where

$$\begin{aligned}c_{eij} &= \int_{\Omega_e}\left(\frac{\partial W_j}{\partial x}\frac{\partial N_i}{\partial x}+\frac{\partial W_j}{\partial y}\frac{\partial N_i}{\partial y}\right)d\Omega, \\ f_{1j} &= \oint_{\partial\Omega_e} W_j\left(\frac{\partial N_i}{\partial x}dy - \frac{\partial N_i}{\partial y}dx\right)\phi_i, \\ f_{2j} &= -\int_{\Omega_e}\left(\frac{\partial N_j}{\partial x}\frac{\partial N_k}{\partial x}+\frac{\partial N_j}{\partial y}\frac{\partial N_k}{\partial y}\right)\Delta\phi_k \,d\Omega, \\ \boldsymbol{\Phi}_e^{\mathrm{T}} &= \{\phi_1 \ \ldots \ \phi_8\} \quad (i, j = 1, 8, k = 1, 3).\end{aligned}$$

Element matrix is then assembled into the global matrix which now has extra terms introduced along the cut:

$$\mathbf{C}\boldsymbol{\Phi} = \mathbf{F}_1 + \mathbf{F}_2 \tag{9}$$

where

$$\begin{aligned}\mathbf{C} &= \sum \mathbf{C}_e, \\ \mathbf{F}_1 &= \sum \mathbf{f}_1, \\ \mathbf{F}_2 &= \sum \mathbf{f}_2.\end{aligned}$$

The extra terms on the right-hand side of the above equation come from the wake and can be assembled in the same manner as described in Hitchings[11] and Shi.[13] Now, however, only those elements inside the wake have contributions. This is because we are dealing with a growing wake

of finite length rather than a steady and infinitely long one as in Hitchings[11] and Shi.[13] The actual form of $\Delta\phi_k$ is given in Section 3.

3. AN EXPLICIT TIME INTEGRATION SCHEME

To obtain a response in the time interval T, it is divided into N time subintervals Δt_n. At time zero the indicial motion is imposed on the aerofoil. Because of the indicial nature of the motion, there is no time for the development of the circulation or for the vortex to be thrown into the wake from time $t=0^-$ to $t=0^+$. Hence, there is no wake or circulation around the aerofoil. At each time instance t_n, a newly shed vortex $\Delta\Gamma_n$ of a length $U_\infty \Delta t_n$ is added to the wake, where $\Delta\Gamma_n$ is decided by the Kutta condition at t_n. Due to the linearity of the problem, the solution at t_n is divided into three parts. The first part, ϕ_0, is non-circulatory, time-independent and is the same as the solution at $t=0$, so it is only solved once at the beginning of the time marching process. The second part, ϕ_1, corresponds to the wake system at t_{n-1} convected a distance $\Delta t_n U_\infty$ downstream during the time interval $[t_{n-1}, t_n]$. The last part, ϕ_2, is associated with the newly shed vortex $\Delta\Gamma_n$. This can be summarized as

$$\begin{aligned} &t=0, && \phi=\phi_0, && \Gamma=\Gamma_0=0,\\ &t=t_{n-1}, && \phi=\phi_{n-1}, && \Gamma=\Gamma_{n-1},\\ &t=t_n, && \phi=\phi_n=\phi_0+\phi_1+\Delta\Gamma_n\phi_2, && \Gamma=\Gamma_{n-1}+\Delta\Gamma_n, \end{aligned} \tag{10}$$

which gives the velocities at time t_n as

$$\begin{aligned} U_n &= U_0+U_1+\Delta\Gamma_n U_2,\\ V_n &= V_0+V_1+\Delta\Gamma_n V_2. \end{aligned} \tag{11}$$

A graphical representation of the velocity potential difference on the wake at different time intervals is given in Figure 4.

ϕ_0, ϕ_1 and ϕ_2 all have to satisfy the Laplace equation. However, the boundary conditions are different for each ϕ:

$$\begin{aligned} &\phi_0\colon \partial\phi/\partial n=U_\infty && \text{on } \partial\Omega_1; && \partial\phi/\partial n=f \text{ on } \partial\Omega_2; && \Delta\phi=0 && \text{on all } s,\\ &\phi_1\colon \partial\phi/\partial \dot{n}=0 && \text{on } \partial\Omega_1; && \partial\phi/\partial n=0 \text{ on } \partial\Omega_2; && \Delta\phi=\text{convected } \Delta\phi_{n-1} && \text{on } 0\le s\le U_\infty t_n,\\ &\phi_2\colon \partial\phi/\partial n=0 && \text{on } \partial\Omega_1; && \partial\phi/\partial n=0 \text{ on } \partial\Omega_2; && \Delta\phi=1{\cdot}0 && \text{on } 0\le s\le U_\infty \Delta t_n, \end{aligned} \tag{12}$$

where f is a known function depending on the form of the indicial motion. At each time step, $\Delta\Gamma_n$ is decided by the Kutta condition of smooth flow at the trailing edge:

$$\Delta\Gamma_n=(V^{TE}-V_0^{TE}-V_1^{TE})/V_2^{TE}, \tag{13}$$

where V^{TE} is a prescribed normal velocity at the trailing edge for a particular mode of indicial motion (see Figure 1). Equation (13) clearly indicates that $\Delta\Gamma_n$ is dimensionless. In this paper, it simply has the magnitude of velocity difference but not its dimension. This is also true for equations (10), (11) and (14).

The pressure at a time instant t_n can be determined by the Bernoulli's theorem:

$$\begin{aligned} p(t_n) &= -\rho(\partial\phi/\partial t+(U^2+V^2)/2)\\ &= -\rho((\phi_n-\phi_{n-1})/(t_n-t_{n-1})+U_0(U_0/2+U_1+\Delta\Gamma_n U_2)+V_0(V_0/2+V_1+\Delta\Gamma_n V_2)). \end{aligned} \tag{14}$$

Note that in equation (14) we have replaced the time derivative of $\partial\phi/\partial t$ by a first-order explicit

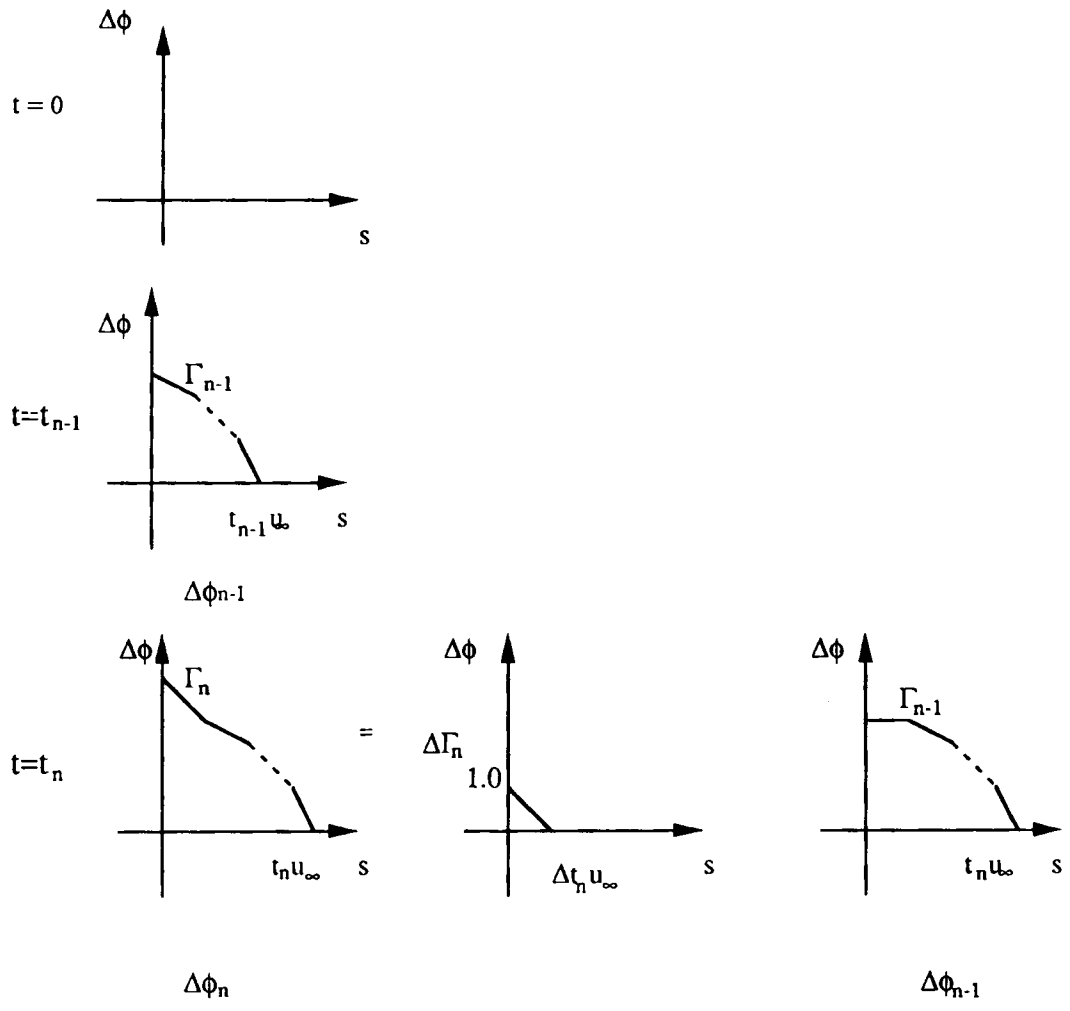

Figure 4. Time integration scheme

backward difference scheme. This is adopted for its simplicity despite of the existence of various other higher-order and implicit difference schemes. The squares of U_1, U_2, V_1 and V_2 have been neglected because of the small disturbance assumption. The second-order terms of mean velocities U_0 and V_0 are nevertheless retained for they might affect the moment resultant in spite of the fact that they are related to the non-circulatory part of the flow and do not influence the lift force.

The pressure can then be integrated along aerofoil surface to get the lift L and the moment M at time t_n:

$$L(t_n) = \int p(t_n)\,\mathrm{d}x, \tag{15}$$

$$M(t_n) = \int p(t_n)((x-x_0)\,\mathrm{d}x - (y-y_0)\,\mathrm{d}y),$$

where (x_0, y_0) is the reference point for the moment and $\int$ means integral along the aerofoil surface. From equation (15), we can get the lift and moment coefficients $C_\ell(t)$ and $C_m(t)$:

$$C_\ell(t) = L(t_n)/(U^2 + V^2)/2,$$
$$C_m(t) = M(t_n)/(U^2 + V^2)/2. \tag{16}$$

This process is repeated until the desired time T is reached.

4. THE SELECTION OF TIME STEP Δt

To capture the smallest detail of the flow transient to the aerofoil motion, a very small time step was used initially ($\Delta t U_\infty / C = 0{\cdot}02$, where C = chord). However, it was found that the lift force oscillates, especially at the beginning of time marching process. It oscillates more violently when the time step was halved (see Figure 5). This seemed to be contradicting to what was expected but a careful examination of the effect of mesh size on the wake shows the reason behind it.

In Figure 5(b) the dashed vertical lines represent the position of element nodes on the wake. Vortices are convected from left to right at a speed U_∞. Each square or discontinuity in the solution curve is a discrete time station in the time marching process. It can be seen that between two nodes the lift falls and rises. If the time increment is too small compared to the distance between two consecutive nodes then it will take many time steps for the wake front to travel from one node to the next, during which the vortices between the two nodes are not known or 'felt' because there is no node there to sense or resolve it. The solution then becomes undefined in that part. This phenomenon is more prominent when the non-dimensionalized time $\Delta t U_\infty / C$ is small, because at the start the wake is short, so that the unaccounted wake front constitutes a substantial part of the whole wake. Consequently, the solution is significantly influenced by it.

Having found this, a much larger time step was employed. As explained previously $\Delta t U_\infty$ should be greater than the node spacing, Δs, to avoid artificial oscillations. In short, the condition $\Delta t U_\infty / \Delta s \geq 1$ should be satisfied. From Figure 6 it is obvious that Δt can be as big as 20 times $\Delta s / U_\infty$ at the start and $\Delta t U_\infty / C \approx 1$ later on without a noticeable deterioration in accuracy. This, of course, is appealing if one has limited computer resources. Consequently, a three-stage time increment scheme is adopted with 0·2, 0·4 and 0·6, respectively, and 20 steps for each increment. The steady state is thought to be reached and thus the time integration is terminated when the lift changes less than 0·1% during a time interval $\Delta t U_\infty / C = 1$.

5. NUMERICAL EXAMPLES AND DISCUSSIONS

5.1. Plate aerofoil

The first two cases are actually related to the numerical modelling of wind tunnel interference. In other words, the influence of the finite dimension of a wind tunnel, especially the height H of the tunnel for a two-dimensional problem, on quantities such as lift and moment. Because of the presence of the wind tunnel walls, the flow direction and streamline curvature will be different from those in air-free conditions. In other words, the circulation around the aerofoil is changed, which is normally referred to as lift interference. At the same time the wind tunnel walls also affect the flow velocity and longitudinal velocity gradient or the velocity potential representing the volume of the aerofoil and the wake, which is the so-called blockage interference effect. These two effects are usually assumed to be independent of each other and alter the characteristics of flow.[15] Since the present finite element analysis truncates an infinite problem domain to a finite one, the

(a)

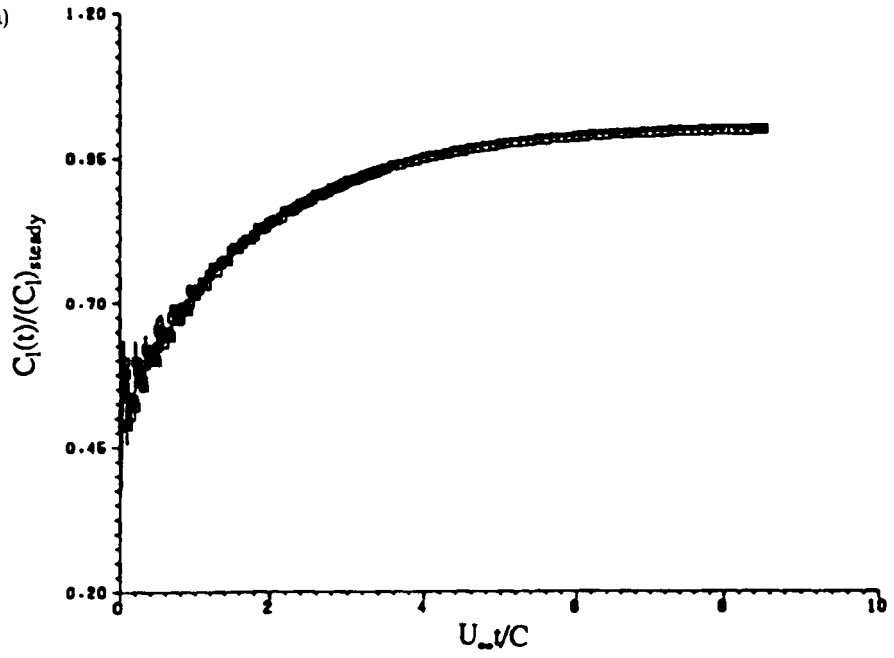

Figure 5(a). Lift oscillation due to too small time step: ——, $\Delta t = 1, 5, 10$; □, $\Delta t = 2, 5, 10$

(b)

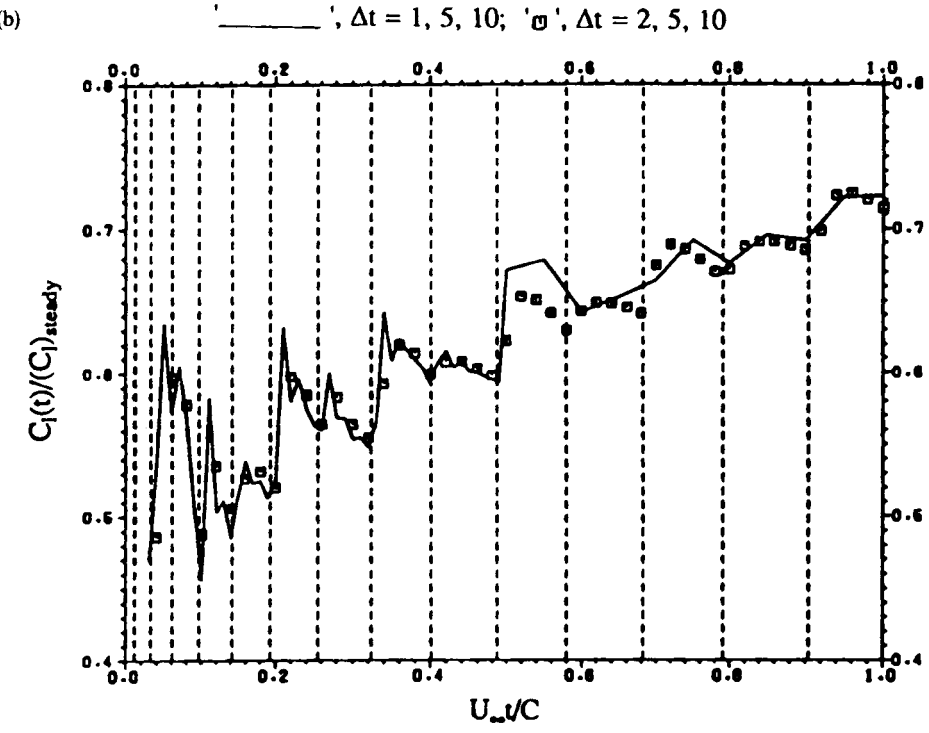

Figure 5(b). Lift oscillation due to small time step (close up): ——, $\Delta t = 1, 5, 10$; □, $\Delta t = 2, 5, 10$

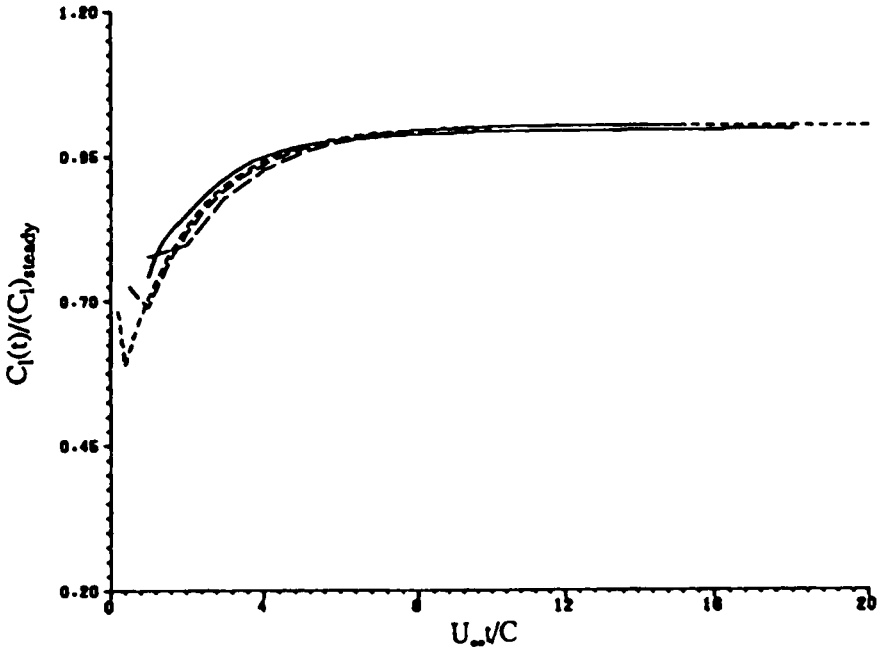

Figure 6. The effect of time step size on solution accuracy: ——, exact; – – – –, $\Delta t = 20$; — — — —, $\Delta t = 50$; – – –, $\Delta t = 100$

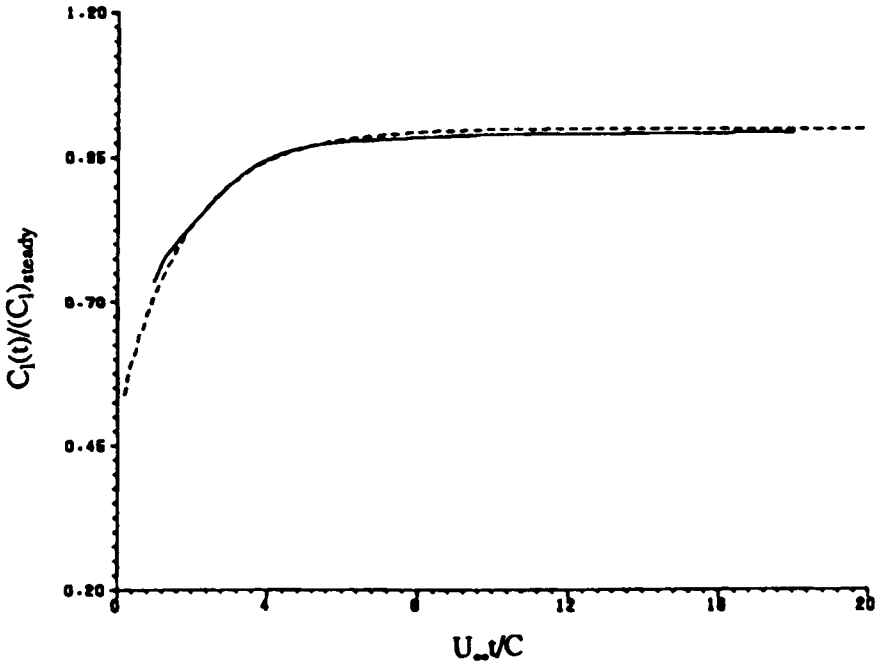

Figure 7. Lift on a plate after a sudden change of incidence $H/C = 2$: ——, Chung[16]; – – – –, finite element

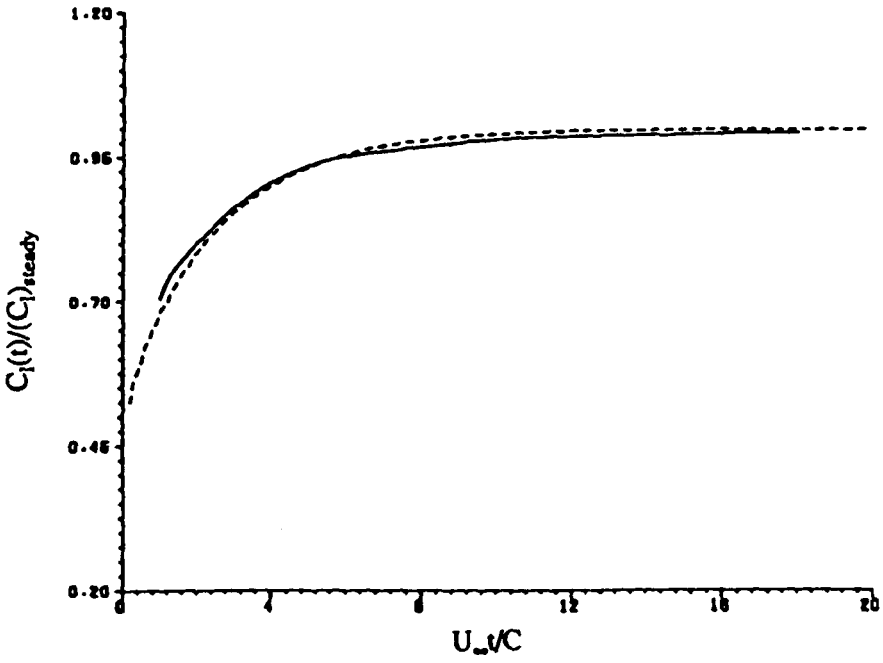

Figure 8. Lift on a plate after a sudden change of incidence $H/C=4$: · — · , Chung[16]; – – –, finite element

boundary condition on the upper and lower mesh boundary is no through flow. This means that the fluid is confined to flow between two parallel artificial barriers, the effect of which is similar to that of wind tunnel walls.

Figures 7 and 8 demonstrate the finite element solution together with those of Chung[16] for indicial lift build-up with $H/C=2$ and 4, respectively. The agreement is very good despite of the fact that for the present formulation the Kutta condition is zero normal velocity rather than zero pressure loading. This confirms the theory that for a cusped trailing edge the Kutta condition can be interpreted as both zero pressure loading and zero normal velocity at the trailing edge. The effect of wind tunnel interference is well simulated as it can be seen that for the smaller H/C value, the lift build-up is faster. We can see that the agreement is better for the case $H/C=2$ than for $H/C=4$, because the same number of elements was used for both, which gave the former a higher mesh density than that of the latter.

The previous two cases correspond to sudden change of incidence. Other modes of indicial motion have also been investigated. The non-dimensionalized lift build-up for a sudden change of heaving rate, pitching rate and control deflection are given in Figures 9, 10 and 11, respectively. Initially, the same mesh for the first two problems was employed and finite element results show considerable discrepancy against the analytical solutions. This is because we are now again dealing with an infinite domain problem. Consequently, a larger mesh was used with the upper and lower mesh boundaries 4C (instead of 2·5C) away above and below the aerofoil. Naturally, the new finite element results are much improved.

5.2. *Von Mises aerofoil*

Numerical tests were also carried out on a symmetric 8·4% thick Von Mises aerofoil (see Figures 12 and 13). As the method employed by Basu[7] allows for wake deformation which is not

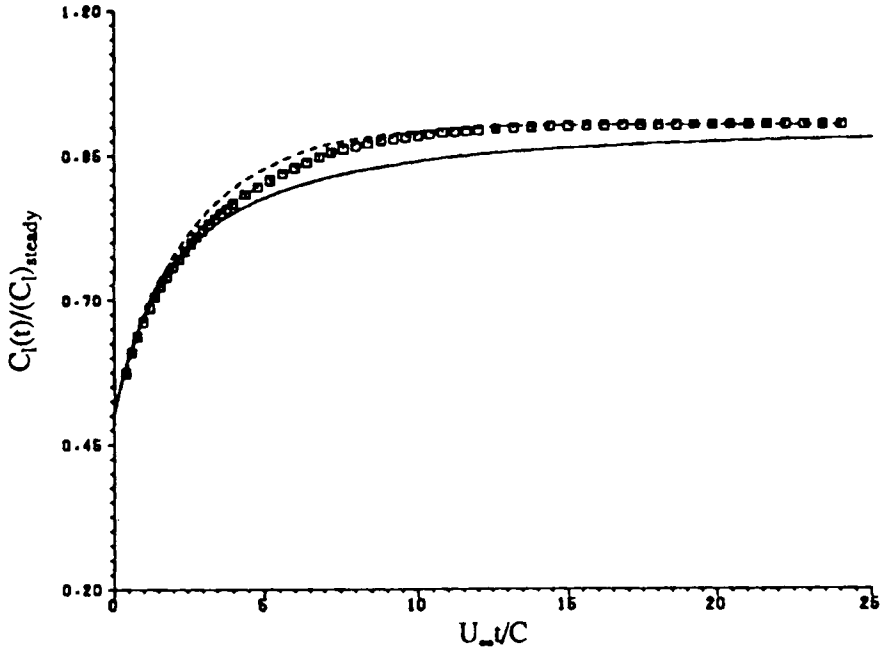

Figure 9. Lift on a plate following a sudden change of heaving rate: ——, analytical; – – – –, finite element (small mesh); □, finite element (large mesh)

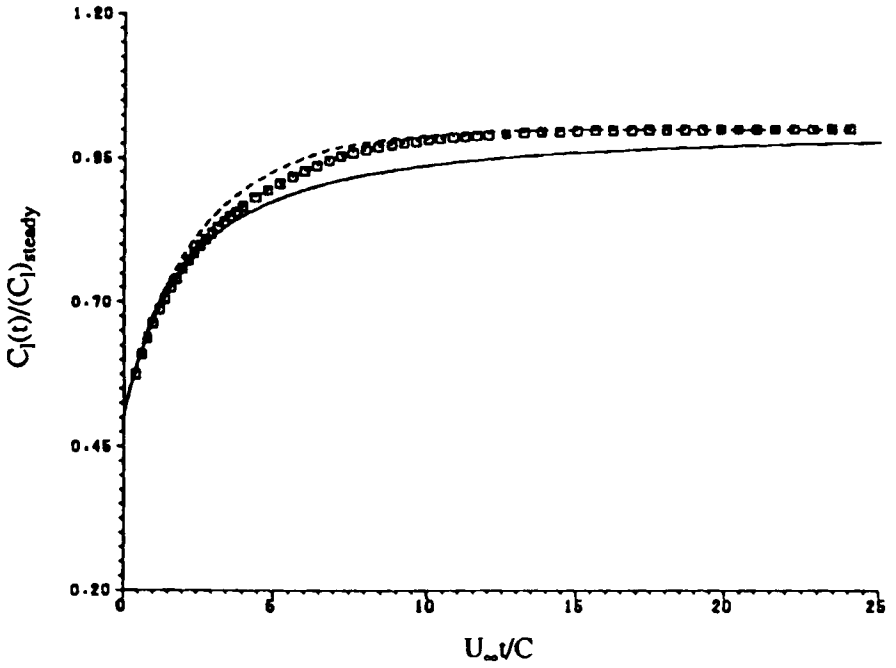

Figure 10. Lift on a plate following a sudden change of pitching rate: ——, analytical; – – – –, finite element (small mesh); □, finite element (large mesh)

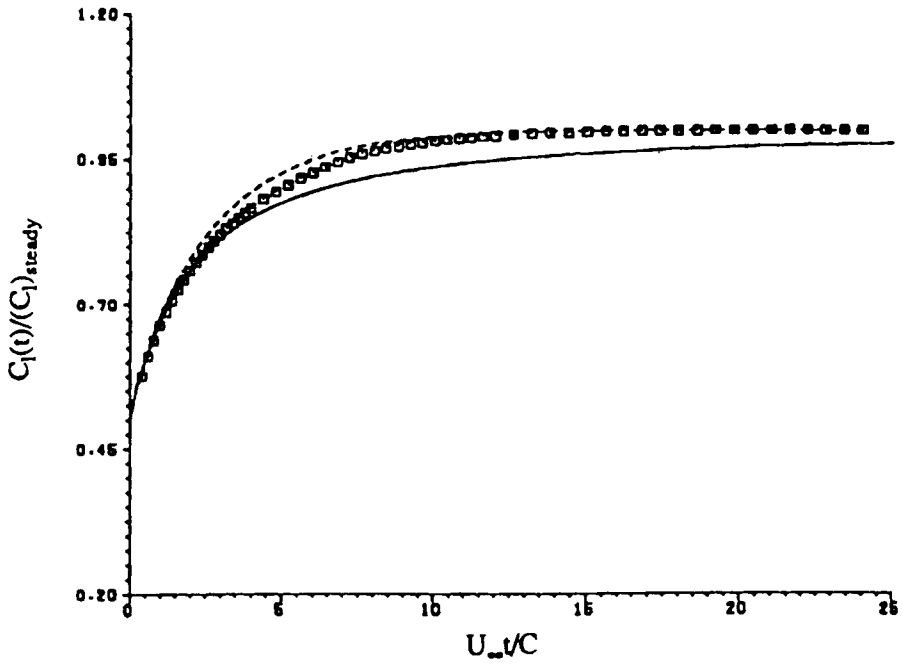

Figure 11. Lift on a plate following a sudden change of control deflection: ——, analytical; – – – –, finite element (small mesh); □, finite element (large mesh)

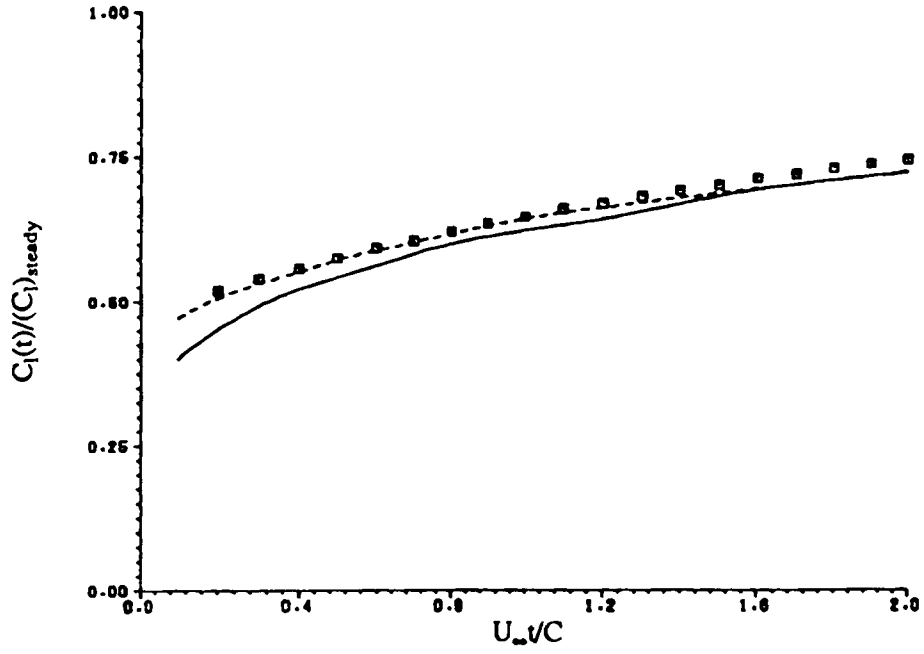

Figure 12. 8·4% thick symmetric Von Mises aerofoil; lift after a sudden change of heaving rate: ——, Basu and Hancock[7]; – – – –, Giesing[6]; □, finite element

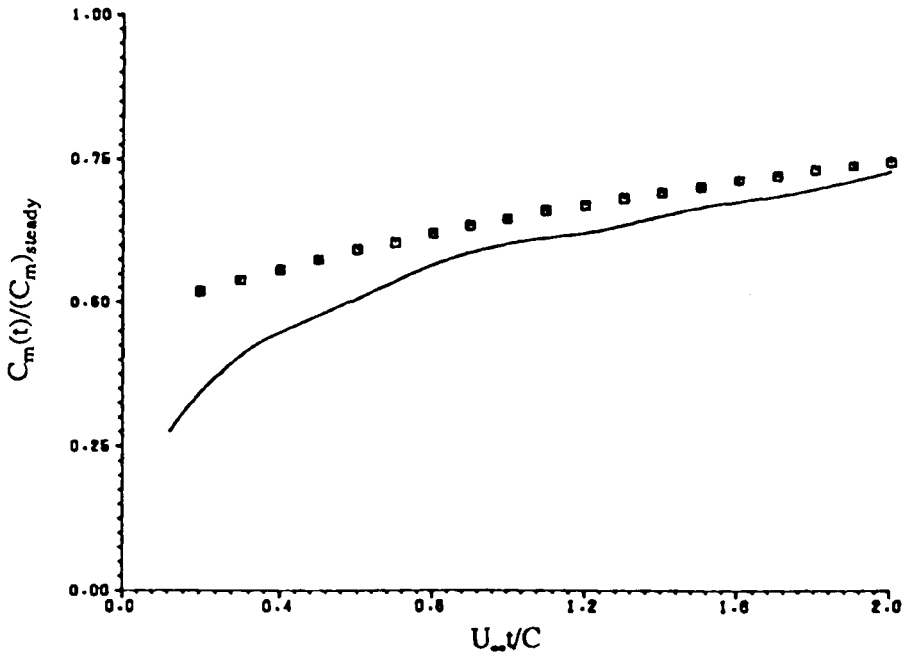

Figure 13. 8·4% thick symmetric Von Mises aerofoil; moment about leading edge after a sudden change of heaving rate: —— , Basu and Hancock[7], □, finite element

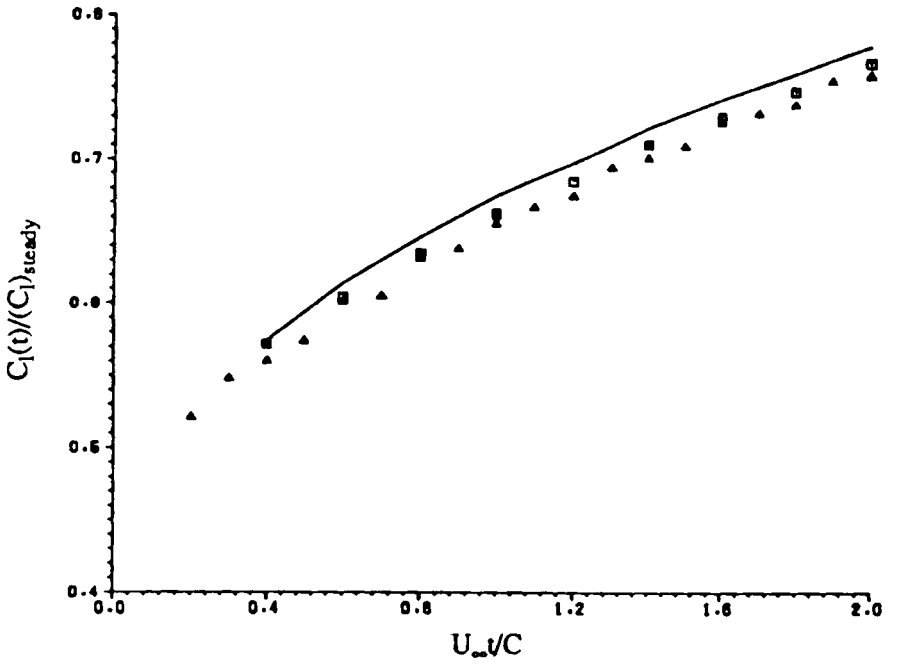

Figure 14. Thickness effect on Wagner function (symmetrical Joukowski aerofoil): ——, plate; □, 5% thick; ▲, 10% thick

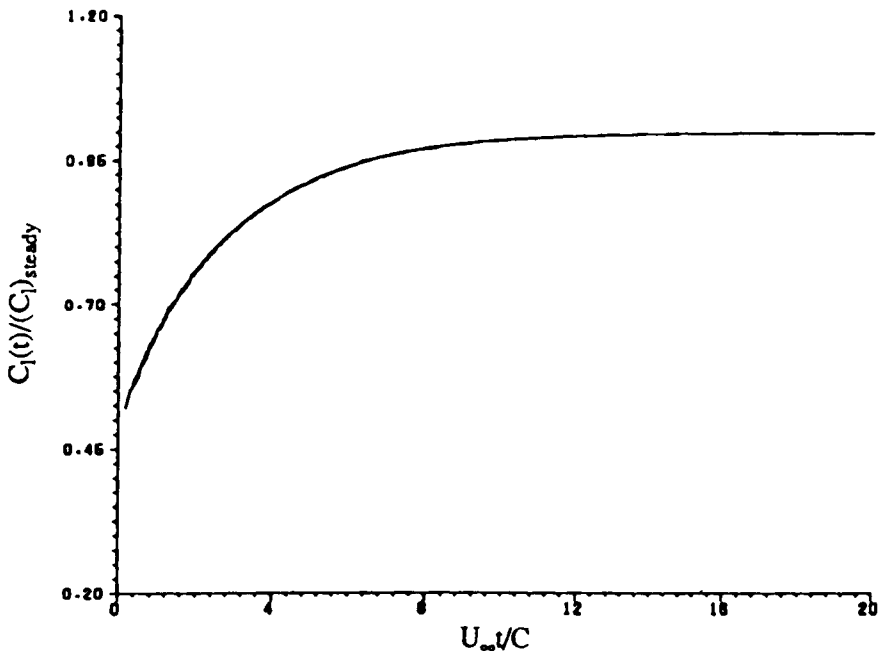

Figure 15. Thickness effect on lift build-up of a 10% thick aerofoil: ——, sudden change of heaving rate; – – – –, sudden change of pitching rate; — — —, sudden change of control deflection

incorporated in the method now used, there is a substantial difference between the two solutions at the initial transient stage. However, when time develops they tend to converge to the same value. This has been well explained by Graham[17] that the initial vortex roll-up has a large influence on the lift and moment build-up in the early stage, but as time goes on its effect decreases and wake can be well represented by a straight line. This is well confirmed by the good agreement between the present solution and that of Giesing,[6] which does not include wake deformation either.

5.3. Thickness effect

The influence of aerofoil thickness on lift build-up was studied on 5 and 10% thick symmetric Joukowski aerofoils. As can be seen in Figure 14 the 10% thick aerofoil takes a longer time to reach a steady state than the 5% thick one and the plate. This has also been observed by Giesing.[6] However, thickness does not affect the lift build-up of different modes of indicial motion. This is illustrated in Figure 15 in which the lift build-up of a 10% thick aerofoil shows little difference for the sudden change of heaving rate, pitching rate and control deflection.

6. CONCLUSION

In this paper a finite element formulation for the transient wake development due to aerofoil indicial motion was proposed. The velocity potential difference was employed to simulate the vortices in the wake. The time stepping scheme was examined with special attention to time increment size, which has to be large enough to allow the wake front travel at least from one node to the next. Numerical experiment showed that $\Delta t U_\infty/C = 0{\cdot}2$ at the beginning and $\Delta t U_\infty/C = 1{\cdot}0$

at later times could be used. Although in this paper the analysis was performed on indicial motion, it is apparent that, as long as the assumption made in Section 2 of this paper holds, then the finite element method proposed can be easily employed for any time transient problem. This can be achieved by simply applying the relevant boundary condition on the aerofoil surface due to its motion at different times.

REFERENCES

1. *ESDU 84020*, 'An introduction to time-dependent aerodynamics of aircraft response, gust and active control', Engineering and Science Data Unit, September 1984.
2. I. E. Garrick, 'On some reciprocal relations in the theory of non-stationery flows', *NACA Report No. 629*, 1936.
3. Y. C. Fung, *The Theory of Aeroelasticity*, Dover, New York, 1969.
4. G. K. Batchelor, *An Introduction to Fluid Dynamics*, Cambridge University Press, Cambridge, 1970.
5. H. Wagner, 'Dynamischer Auftrieb Von Tragflache, *'Zeitschrift fuer Angewandtle Mathmatik und Mechanik*, **5**, 17 (1925).
6. J. P. Giesing, 'Nonlinear two-dimensional unsteady flow with lift', *J. Aircraft*, **5**, 135 (1968).
7. B. C. Basu and G. J. Hancock, 'The unsteady motion of a two-dimensional aerofoil in incompressible inviscid flow', *J. Fluid Mech.*, **87**, 159 (1978).
8. J. L. Hess and A. M. O. Smith, 'Calculation of potential flow about arbitary bodies', *Prog. Aeronaut. Sci.*, **8**, 1 (1966).
9. I. Harari and T. J. R. Hughes, 'A cost comparison of boundary element and finite element method for problem of time-harmonic acoustics', *Comput. methods appl. mech. eng.*, **97**, 77–102 (1992).
10. O. C. Zienkiewicz, R. Loehner, K. Morgan and S. Nakazawa, 'Finite elements in fluid mechanics — a decade of progress', in R. H. Gallagher and O. C. Zienkiewicz (eds), *Finite Element in Fluids*, Wiley, New York, Vol. 5, 1984, pp. 1–26.
11. D. Hitchings and J. Shi, 'Calculation of flutter derivatives and speed by finite element method', *Proc. Int. Conf. on Aero-HydroElasticity*, Prague, December 1989.
12. J. Shi and D. Hitchings, 'An accurate finite element method for 2D airfoil problems', in G. N. Pande and J. Middleton (eds), *Numerical Method: Theory and Application*, Elsevier Applied Science, Swansea, 1990, pp. 970–977.
13. J. Shi and D. Hitchings, 'Finite element analysis of an airfoil immersed in a sinusoidal gust', *Proc. 12th Int. Conf. on Numerical Methods for Fluid Dynamics*, Oxford, July 1990.
14. O. C. Zienkiewicz, *The Finite Element Method*, 3rd edn, McGraw-Hill, New York, 1977.
15. *ESDU 76028*, 'Lift interference and blockage corrections for 2D subsonic flow in ventilated and closed wind tunnels', Engineering and Science Data Unit, November 1976.
16. C. W. Chung and G. J. Hancock, 'Wind tunnel interference on unsteady two-dimensional aerofoil motions in low speed flows', *Aeronaut. J.*, **V95**, 115–121, (March, 1988).
17. J. M. R. Graham, 'The lift on an airfoil in starting flow', *J. Fluid Mech.*, **133**, 413 (1983).